Materials Research. 2025; 28:e20240456
DOI: https://doi.org/10.1590/1980-5373-MR-2024-0456

Effect of Calcium Addition Timing to Liquid Steel on Inclusion Modification of Steel Heavy Plates

***Pedro Henrique Resende Vaz de Melo*[a]*, Marlon José dos Anjos Silva[a], Rodrigo Madrona Dias[a],**
***Wagner Viana Bielefeldt*[b], André Luiz Vasconcellos da Costa e Silva[c]**

[a]*Usinas Siderúrgicas de Minas Gerais (Usiminas), Avenida Pero Vaz de Caminha, 274, 35160-238, Ipatinga, MG, Brasil.*
[b]*Universidade Federal do Rio Grande do Sul (UFRGS), Departamento de Metalurgia, Av. Bento Goncalves, 9500, 91501-970, Porto Alegre, RS, Brasil.*
[c]*Universidade Federal Fluminense (UFF), Escola de Engenharia Industrial e Metalúrgica de Volta Redonda, Av. dos Trabalhadores, 420, 27225-125, Volta Redonda, RJ, Brasil.*

Received: October 08, 2024; Revised: December 10, 2024; Accepted: February 02, 2025

Calcium addition to steels normally aims at modifying inclusions to improve castability and cleanliness. This study investigated the inclusion modification efficiency in liquid steel for three conditions varying injection timing: all Ca after RH degasser, all Ca before RH degasser and split addition. Six industrial heats were produced at Usiminas Steelworks, two for each condition. The heats were sampled for automated SEM/EDS inclusion analysis and total oxygen and the results compared to computational thermodynamics simulations. Inclusion modification was most efficient for the split addition condition. This condition was the closest to the calculated castability window, resulting in low inclusion density, a higher percentage of liquid inclusions during casting and lower CaS formation. Furthermore, computational thermodynamic simulations and inclusion analysis presented good agreement. These findings not only enhance the understanding of calcium treatment in steel production but also provide practical insights for optimizing the calcium addition process.

Keywords: *Steel cleanliness, Calcium treatment, Computational thermodynamics, Secondary refining.*

1. Introduction

Calcium addition in steels aims to modify inclusions, such as Al_2O_3, which are deleterious to steel castability and product quality. The objective of this addition is to form liquid inclusions at liquid steel temperatures, minimizing their adherence and accumulation on the internal surfaces of the continuous casting valves, thus preventing nozzle clogging. Furthermore, this may facilitate inclusion coalescence and their removal to the slag, providing greater cleanliness to the steel[1,2].

Calcium treatment is a traditional practice in steelmaking and the subject of extensive study, most of them have been reviewed by Ren et al.[2], Costa e Silva[3] and Pindar and Pande[4]. However, challenges remain in the process, such as the amount to be added, timing and speed of addition and calcium yield[5-7]. Steel chemical composition and temperature are the main variables influencing the ideal Ca addition, making each heat a specific case and highlighting the theme's complexity[8,9].

Longer rinsing times result in a higher inclusions removal from the steel bath, especially those with smaller dimensions, that can coalesce and be carried by the stirred melt or by bubbles to the slag[10,11]. However, due to the need of melt shop synchronism and for productivity reasons, the heats processing time is limited. Thus, aiming to increase the flotation time after calcium treatment, anticipating the moment of addition may enable the removal of more inclusions to the slag and improve steel cleanliness. Longer holding times after injection, however, may result in Ca loss, known as fading, and affect the alloy yield[12]. Therefore, these two factors must be pondered when an early versus later addition is considered.

The aim of this study was to compare the inclusion modification efficiency by calcium addition for three timings of injection, namely: all calcium added after Ruhrstahl-Heraeus (RH) degasser (standard condition), all added before RH degasser and split addition. Beyond deepening discussions about Ca treatment and injection timing, the results can be used in future work to improve the castability and cleanliness of heavy plates produced at Usiminas Steelworks.

2. Materials and Methods

Heavy plate steels evaluated in this study are low carbon, silicon-aluminum killed, and calcium treated. At Usiminas these steels are produced following the route: Basic Oxygen Furnace (BOF) → Ladle Furnace (LF) or Composition Adjustment by Sealed Argon Bubbling and Oxygen Blowing (CAS-OB) → RH degasser → Continuous Casting[13], as shown in Figure 1.

*e-mail: pedrovazdemelo21@hotmail.com

The standard addition moment of Ca for these steels is after RH degasser just before ladle release for continuous casting. In this study, it was proposed to change the calcium addition timing to provide more time for inclusions flotation. Beyond the standard addition condition (Condition 1), industrial tests were proposed with split addition, before and after RH treatment (Condition 2), and the total addition of Ca only before RH (Condition 3). Six heats were evaluated, two for each condition. The total amount of calcium silicide (CaSi) alloy added was 110 kg per heat, with each heat weighing approximately 165 tons.

Commercial samplers without deoxidizer were used to avoid reactions with oxide inclusions, targets of the study, as proposed by Kaushik et al.[14] Tundish samplings were performed at 50% of ladle casting. The samples were taken to Usiminas Research and Development Center for automated Scanning Electron Microscope/Energy Dispersive X-Ray Spectroscopy (SEM/EDS) inclusion analysis.

The INCA Feature software (Oxford instruments, UK), a resource installed in SEM EVO 50, was used for the analysis of inclusions considering particles over than 3 µm. Analysis consists of an automated scan of the sample's entire surface, in which the identified inclusions are characterized in terms of dimensions and chemical composition via EDS. The samples for inclusion analysis were taken from the same position in the samplers and the examined surface area was about 120 mm^2. The main analytical parameters of the automated scan were magnification of 500 X, accelerating voltage of 20 kV, working distance of 8.5 mm and image resolution of 1024 x 832 pixels.

In the EDS results, points identified as inclusions with more than 95% Fe were disregarded to filter out pore interference, as suggested by Dogan et al.[15] The remaining EDS results were then normalized, disregarding the Fe element, assuming this comes for the steel ferritic matrix. The inclusion classification followed the rules described in Table 1. The classification of calcium aluminates was on the pseudobinary diagram CaO x Al_2O_3 at a temperature of 1500ºC. Other inclusion classes, such as spinels, calcium sulfides, and silicates, were adapted from the criteria proposed by Alves et al.[16] with some modifications. An independent spreadsheet, separate from INCA Feature, was developed

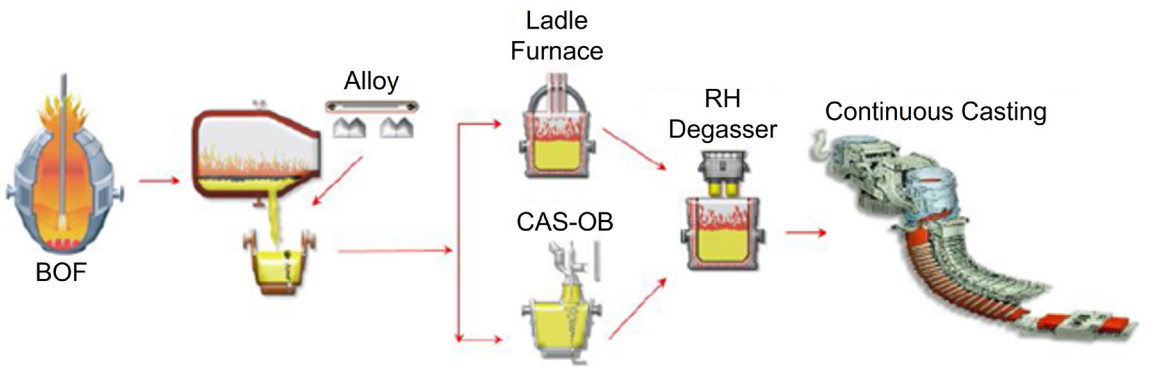

Figure 1. Steel production route for heavy plates at Usiminas steelworks[8].

Table 1. Classification rules used on the INCA Feature results to classify the inclusions found in the solidified steel samples.

Chemical class	Classification rule (Element content in wt%)
Spinel	[Mg/(Al+Mg+Ca)] > 0.15; (Al + Mg) > 30
Calcium sulfide (CaS)	Ca > 20; S > 20
CaAl solid (CaO) – CaO + C3A	Ca + Al >= 30; Al < 20.11
Multi-phase(solid(s)+liquid) + C3A	Ca + Al >= 30; 20.11 < Al < 23.81
Liquid Oxides	Ca + Al >= 30; 23.81 < Al < 29.11
Multi-phase(solid(s)+liquid) + CA	Ca + Al >= 30; 29.11 < Al < 34.40
CaAl solid (Al_2O_3) – CA + CA2	Ca + Al >= 30; 34.40 < Al < 41.28
CaAl solid (Al_2O_3) – CA2 + CA6	Ca + Al >= 30; 41.28 < Al < 48.69
CaAl solid (Al_2O_3) – CA6 + Al_2O_3	Ca + Al >= 30; 48.69 < Al < 52.93
Al_2O_3	Ca + Al >= 30; 52.93 < Al
Silicate	Si > 37
Non-classified	Does not meet any criteria

to implement the classification system. However, the classification currently lacks specific classes and criteria to account for manganese sulfides (MnS), mixed (Ca,Mn)S inclusions, and alumino-silicates, representing an opportunity for future development.

An indirect method of evaluating the inclusion amount in steel is through total oxygen analysis[17]. Oxygen may be dissolved in steel or in the form of oxides (inclusions). As the amount of dissolved oxygen is much lower than the quantity of oxides in well deoxidized steel, the total oxygen may be considered an indicator of the inclusions level in the steel. Tundish samples were selected for total oxygen evaluation, properly prepared, and analyzed in G8+MS GALILEO BRUKER equipment.

After monitoring and sampling industrial heats, computational thermodynamic calculations were performed to determine the range of calcium content at which the inclusions are fully liquid, named "castability window", and how close the actual heats were to these windows. The types of inclusions formed were also calculated for each condition. For simulations, the Thermo-Calc (TC) software (version 2022a) was used together with SLAG4 database. The contents of C, Al, S, Ca, Mn, Si, O_{total} and temperature were used as input data, all data collected at tundish. Table 2 shows the exact chemical composition and temperature of each heat used for the thermodynamic calculations.

The "Equilibrium Calculator" module in Thermo-Calc was employed, using a "one axis" calculation method, which varies a single condition—in this case, calcium content (0–50 ppm). Aluminum content was also varied between 200 and 450 ppm to evaluate its effect on inclusion formation. Saturation curves were then determined, defining the boundaries of the castability window for inclusions such as CaS and calcium aluminates, and plotted on a binary Ca-Al phase diagram.

The results of automated inclusions analysis, total oxygen and calculated castability windows were used to evaluate and compare the efficiency of calcium treatment for the three conditions, as discussed in the following section.

3. Results and Discussion

3.1. Condition 1 – standard addition

Castability windows for condition 1 heats are shown in Figure 2. This figure is based on the diagram proposed by Holappa et al.[8] and Leão et al.[9] The window is displayed as a function of variation of Ca and Al contents. The interval between the solid calcium aluminates (CA) and CaS saturation lines is the field where inclusions are liquid at continuous casting temperatures. The black triangles represent the position of each heat in relation to the castability window.

For the two heats of condition 1, the chemical compositions position the chemical analysis results above the CaS formation line. The formation of solid CaS indicates excessive calcium additions[18,19].

Figure 2 also shows the effect of Al on the CA and CaS saturation lines of the liquid oxide mixture. An increase in Al

Table 2. Chemical composition (mass %) of liquid steel in tundish samples and temperatures considered for computational thermodynamic calculations of castability windows.

Condition	Heat	C	Al	S	Ca	Mn	Si	O_{total}	Tundish T[ºC]
1	A	0.150	0.034	0.006	0.0028	1.36	0.28	0.0015	1537
1	B	0.162	0.038	0.003	0.0021	1.34	0.35	0.0017	1535
2	A	0.157	0.035	0.002	0.0015	1.36	0.30	0.0017	1538
2	B	0.167	0.040	0.003	0.0014	1.36	0.34	0.0012	1535
3	A	0.162	0.038	0.006	0.0004	1.35	0.31	0.0010	1539
3	B	0.172	0.036	0.005	0.0003	1.38	0.36	0.0013	1537

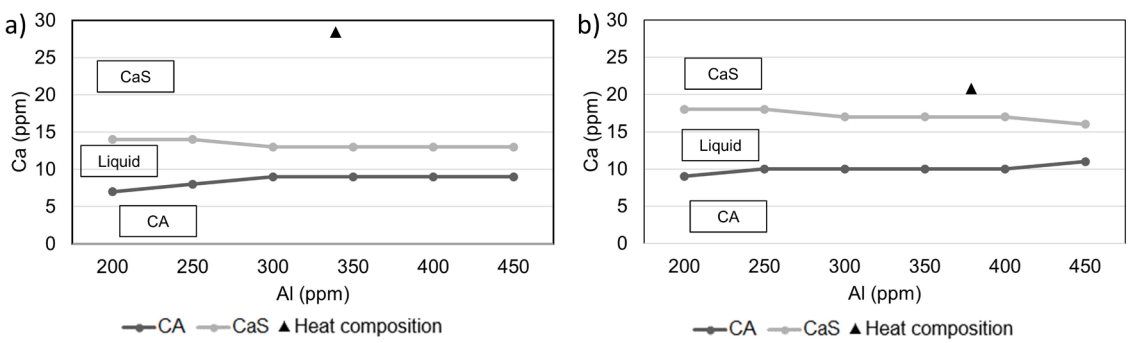

Figure 2. Castability windows for (a) heat 1A and (b) heat 1B, calculated with TC+SLAG4. Steel composition and temperature data at Table 2. For heat 1A, the O_{total} content was 0.0015% and the S content was 0.006%. For heat 1B, the O_{total} content was 0.0017% and the S content was 0.003%.

content results in a narrower castability window, as previously observed by Leão et al.[9] Heat 1A presented a castability window for lower Ca intervals and was narrower than that of heat 1B. This is due to heat 1A having a lower total oxygen content than heat 1B, i.e., a lower amount of oxide inclusions. When less oxides are present, a lower amount of calcium is needed to modify them. This agrees with literature.[8] The higher sulfur content in heat 1A compared to heat 1B was responsible for shifting down the CaS saturation line.

Table 3 presents the percentage of inclusions formed for heats in condition 1, calculated via computational thermodynamics using the data of Table 2 as equilibrium conditions. The simulations indicate that solid inclusions consist solely of of CaS, while the remaining inclusions are liquid oxides for both heats. The formation of CaS is strongly dependent on the sulfur content in the steel. The CaS content calculated for heat 1A was higher than for heat 1B. Furthermore, heat 1A presents lower liquid inclusion content. Further away from the saturation line, the content of liquid decreases and that of CaS increases in all calculations. When considering the liquid/solid inclusion ratio for oxides only, as shown in Table 3, 100% of oxide inclusions are liquid for heats 1A and 1B. The higher S and Ca contents in heat 1A are the main factors causing this behavior.

These factors may also be seen in Figure 3, where the CaS/(CaS + liquid inclusions) ratio was calculated as a function of Ca content. A ratio greater than zero indicates CaS saturation. The actual Ca content of both heats is plotted in Figure 3. In both cases, the points suggesting excessive Ca additions.

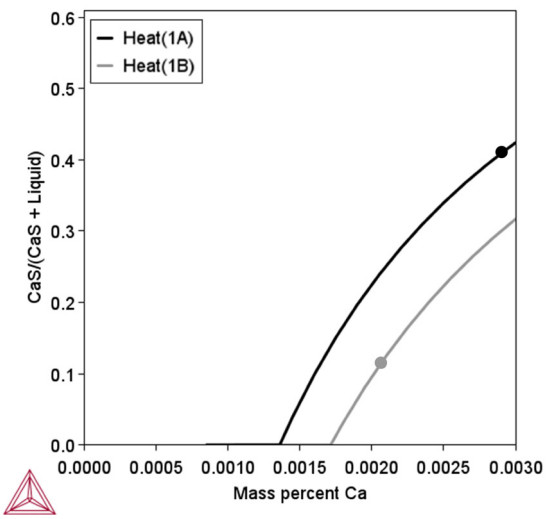

Figure 3. CaS/(CaS + Liquid inclusions) ratio in function of Ca content for condition 1 heats, calculated with TC+SLAG4. Steel composition and temperature data at Table 2.

Figure 4 shows inclusion classification by automated analysis in INCA Feature for heats 1A and 1B. Calcium sulfide inclusions in tundish samples represented 28% and 37% in heats 1A and 1B, respectively. These results are consistent with computational thermodynamic calculations and indicate the excess of added calcium. Liquid oxides and multi-phase (solid(s)+liquid) also had a representative percentage.

3.2. Condition 2 – split calcium addition

Figure 5 shows castability windows as a function of Ca and Al contents variation for these heats. This graph is interpreted in the same way as Figure 2. Heat 2A was positioned between the CA and CaS saturation lines, indicating the formation of fully liquid inclusions and adequate calcium treatment. Heat 2B exceeds the CaS saturation line. Even with similar Ca content among condition 2 heats, the calcium sulfide was formed by the anticipation of saturation line in function of minor O_{total} and higher S content for heat 2B. In this case, the Ca obtained should be between 7 and 11 ppm. Another factor that would bring heat 2B closer to the fully liquid formation field would be a decrease in Al content. The position of the lower CA/Liquid line is mainly influenced by O_{total}, while the upper Liquid/CaS line depends mostly on the sulfur content, which explains the shift observed in the different heats.

Figure 6 shows the influence of total oxygen in CaS formation by plotting a binary phase diagram of total oxygen and aluminum. In the figure, it can be seen the saturation lines for the Ca sulfide and solid calcium aluminate (CA). In fields, liquid inclusions are represented as SLAG. Heats 2A and 2B showed similar CaS saturation lines and overlapped on the graph. The castability window is the area between the saturation lines and is narrower for heat 2B than 2A, as seen in Figure 5. The position of each heat is identified on the diagram. Due to the smaller O_{total}, heat 2B reached the CaS field, while heat 2A achieved the liquid field.

Table 4 shows formed inclusions calculations by computational thermodynamics. It indicated 100% of liquid inclusions for heat 2A, reaching the castability window, while for heat 2B, most formation of liquid inclusions (89%) and the minority of CaS (11%). Regarding only the oxide inclusions, the liquid/solid ratio, presented 100% liquid inclusions for both heats (2A and 2B).

Figure 7 shows CaS/(CaS + liquid inclusions) ratio in function of Ca content for condition 2 heats, calculated with TC+SLAG4. Steel composition and temperature data at Table 2. The ratio between CaS and CaS + liquid inclusion was equal to zero for heat 2A and there was a ratio greater than zero for heat 2B, as an indication of CaS formation.

Table 3. Types and percentages of inclusions, as well as the Liquid/Solid ratio in oxide inclusions, calculated with TC+SLAG4 for condition 1. Steel composition and temperature data at Table 2.

Condition	Heat	Al_2O_3 (%)	CA6 (%)	CA2 (%)	CA (%)	Liquid (%)	CaS (%)	Liquid/Solid in oxide inclusions (%)
1	A	-	-	-	-	57	43	100
1	B	-	-	-	-	89	11	100

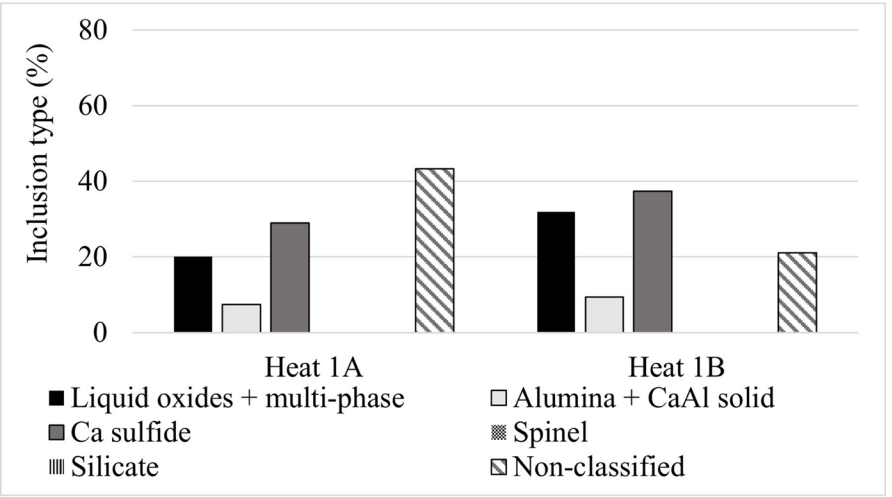

Figure 4. Distribution of inclusion types in tundish samples of heats 1A and 1B.

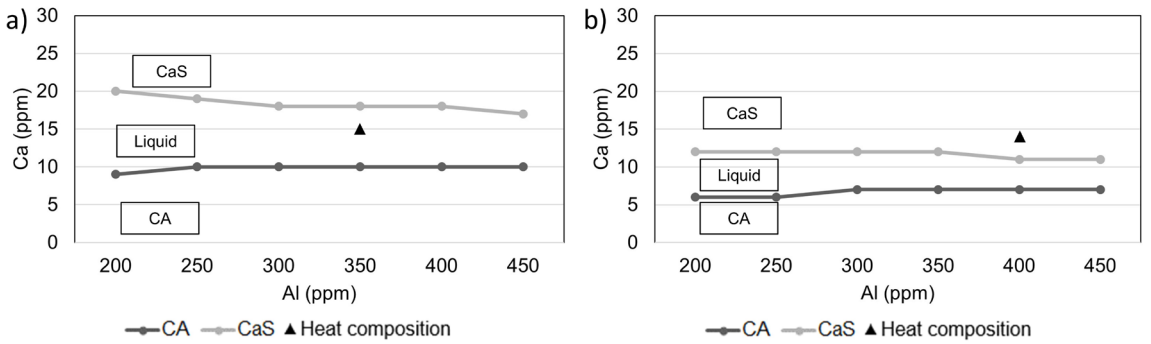

Figure 5. Castability windows for (a) heat 2A and (b) heat 2B, calculated with TC+SLAG4. Steel composition and temperature data at Table 2. For heat 2A, the O_{total} content was 0.0017% and the S content was 0.002%. For heat 2B, the O_{total} content was 0.0012% and the S content was 0.003%.

Table 4. Types and percentages of inclusions, as well as the Liquid/Solid ratio in oxide inclusions, calculated with TC+SLAG4 for condition 2. Steel composition and temperature data at Table 2.

Condition	Heat	Al_2O_3 (%)	CA6 (%)	CA2 (%)	CA (%)	Liquid (%)	CaS (%)	Liquid/Solid in oxide inclusions (%)
2	A	-	-	-	-	100	-	100
2	B	-	-	-	-	89	11	100

Figure 8 shows distribution of inclusion types in tundish samples of heats 2A and 2B. For heat 2A sample, inclusions were mainly composed of liquid oxides or multi-phase, achieving the modifying inclusions aimed, as indicated by the thermodynamic calculations. As for calcium sulfides, they were not significantly formed during the process, representing about 4.5% in the tundish sample. For heat 2B, the solid Al_2O_3 and calcium aluminate inclusions were higher than liquid and multi-phase inclusions, contrary to heat 2A, probably because the castability window was not reached. CaS inclusions were not significant, as in heat 2A, reaching a maximum of 3% in the tundish, contrary to thermodynamic calculations. The CaS formation was probably impaired by the heat low sulfur content (30 ppm).

3.3. Condition 3 – calcium addition only before RH

Figure 9 shows castability windows for (a) heat 3A and (b) heat 3B, calculated with TC+SLAG4. Steel composition and temperature data at Table 2. The two heats of condition 3 were positioned below the CA2 and CA saturation line in Figure 9, having Ca contents lower than 5 ppm. Graphics interpretation follows the logic of previous conditions (Figures 2 and 5). Addition before RH incurred an element

content decrease in the tundish sample. Thus, the way in which calcium was injected was not sufficient for liquid oxides formation. To reach the liquid field, it would be necessary between 5 and 8 ppm in heat 3A and between 7 and 12 ppm in heat 3B.

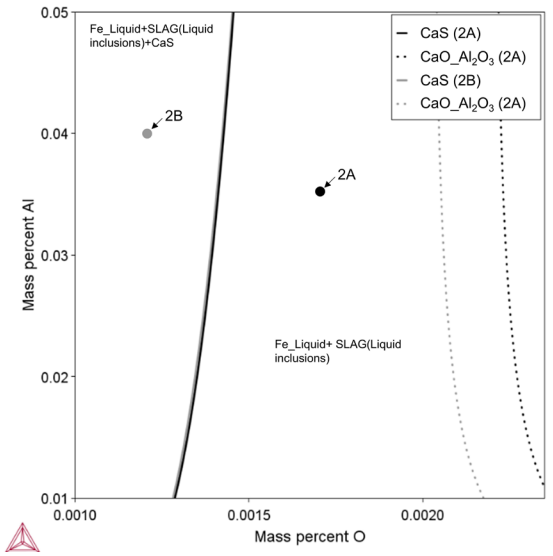

Figure 6. Binary phase diagram total oxygen vs aluminum for heats 2A and 2B, showing the saturation lines for CaS and calcium aluminate. Liquid inclusions are labeled as Fe_liquid+SLAG. Heat 2B reaches the CaS field due to lower O_{total} content, while heat 2A remains in the liquid field.

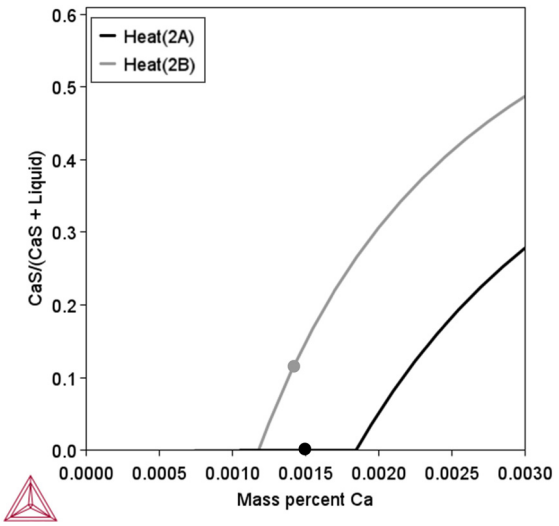

Figure 7. CaS/(CaS + liquid inclusions) ratio in function of Ca content for condition 2 heats, calculated with TC+SLAG4. Steel composition and temperature data at Table 2.

Table 5 shows inclusion formation calculated by TC+SLAG4. It presented the calcium aluminates CA2 and CA for heat 3A and, for heat 3B, CA6 and CA2. In both cases, there would be no formation of liquid inclusions and CaS, which implies a ratio of liquid/solid oxide inclusions equal to zero.

Figure 10 shows the CaS/CaS+liquid inclusion ratio for condition 3 heats. This ratio is only meaningful when at least one of the inclusion types involved—either liquid inclusions or CaS—is present. At lower calcium contents, such as in heats 3A and 3B, this ratio cannot be calculated because these inclusion types are not formed. Nevertheless, the points were plotted on the graph to reaffirm the non-formation of CaS, even for heat 3A, which presented the lowest CaS saturation among all six heats investigated (8 ppm of Ca). This lower saturation point is likely influenced by the exceptionally high S:O ratio of 6:1 in this heat, resulting from the minor O_{total} and higher S content compared to the other heats.

Figure 11 shows distribution of inclusion types in tundish samples of heats 3A and 3B.

Automated inclusion analysis revealed that, in heat 3A, most of the inclusions were classified as solid calcium aluminates (CA + CA2). In heat 3B, these inclusion types represented 4% and solid alumina and CA were 67% of the total. CaS inclusions were not detected. The significant solid calcium aluminates fraction and the low formation of CaS in the tundish for condition 3 heats corroborate with TC+SLAG4 results.

3.4. Ca/O_{total} ratio in steel

Bannenberg[18] used the Ca/O_{total} ratio as an empirical index of steel castability and proposed an optimal value of $0.6 < Ca/O_{total} < 1.0$. As a way of comparison, the Ca/O_{total} ratio is shown in Figure 12 for tundish samples of the present heats.

The relation is strongly influenced by the Ca content since the variation in total oxygen is low between the heats in various processing conditions. Condition 1 heats showed a ratio of 1.78 and 1.35, both above the ratio proposed by Bannenberg[18]. For split addition condition, the ratio for heats 2A and 2B were 0.86 and 1.10, respectively. These are close to the adequate range of castability. When the total addition of calcium was performed before RH, the ratio was below 0.4 for both heats, due to low Ca content in samples.

Here it is important to emphasize that the relationship proposed by Bannenberg[18] does not provide information about the presence of CaS. So, depending on the S content in the steel, this relationship can actually lead to a significant formation of CaS. This relationship also does not predict the influence of the presence of MgO in the inclusions and the formation of $MgO.Al_2O_3$ inclusions. Therefore, the use of this relationship must be combined with the use of

Table 5. Types and percentage of inclusions, as well as the Liquid/Solid ratio in oxide inclusions, calculated with TC+SLAG4 for condition 3. Steel composition and temperature data at Table 2.

Condition	Heat	Al_2O_3 (%)	CA6 (%)	CA2 (%)	CA (%)	Liquid (%)	CaS (%)	Liquid/Solid in oxide inclusions (%)
3	A	-	-	52	48	-	-	0
3	B	-	30	70	-	-	-	0

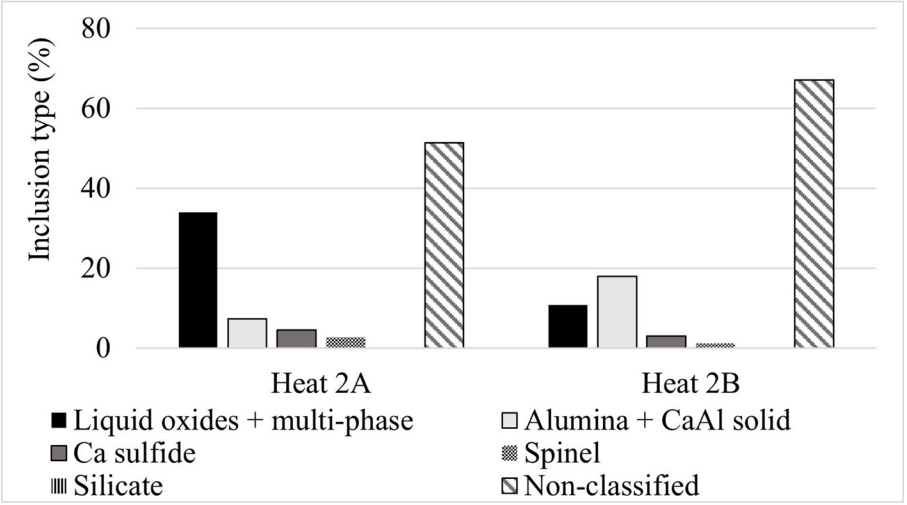

Figure 8. Distribution of inclusion types in tundish samples of heats 2A and 2B.

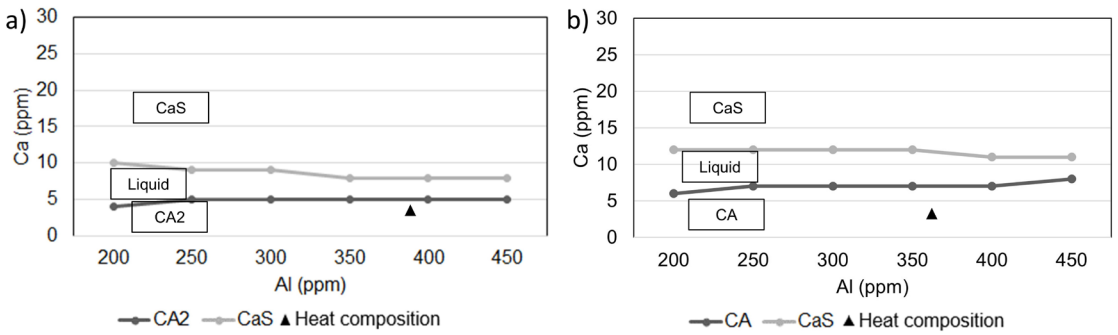

Figure 9. Castability windows for (a) heat 3A and (b) heat 3B, calculated with TC+SLAG4. Steel composition and temperature data at Table 2. For heat 3A, the O_{total} content was 0.0010% and the S content was 0.006%. For heat 3B, the O_{total} content was 0.0013% and the S content was 0.005%.

computational thermodynamics, which provides complete information on the composition of the inclusions based on the composition of the steel and the temperature.

3.5. Inclusion density

With respect to inclusion number density (number/mm^2), condition 2 led to the best results (heats 2A and 2B), as shown in Figure 13. This may be due to the longer time for inclusion removal, starting from the first calcium addition, as well as the absence of significant decrease in calcium content, due to the second addition. Furthermore, some authors propose that the agglomeration of liquid and multi-phase inclusions is more favorable, which enhances their removal from the steel bath [20,21]. It is important to note that the inclusion density values in this analysis also considered non-classified inclusions. Thus, the split addition was the most efficient in modifying inclusions among the three tested conditions.

3.6. General discussion

After calcium addition in heats 1A and 1B (condition 1), most inclusions are composed of solid phases, either CaO +

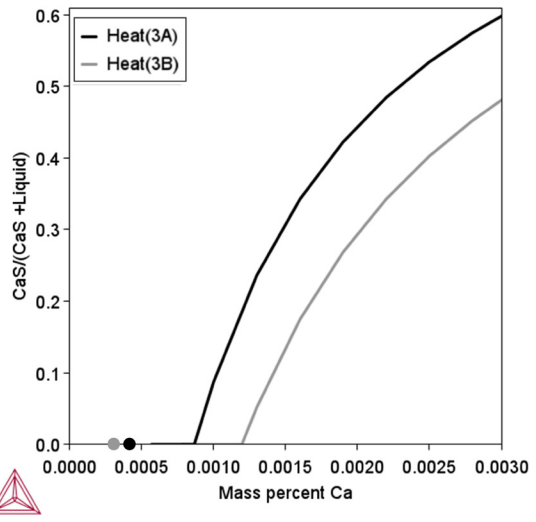

Figure 10. CaS/(CaS + liquid inclusions) ratio in function of Ca content for condition 3 heats, calculated with TC+SLAG4. Steel composition and temperature data at Table 2.

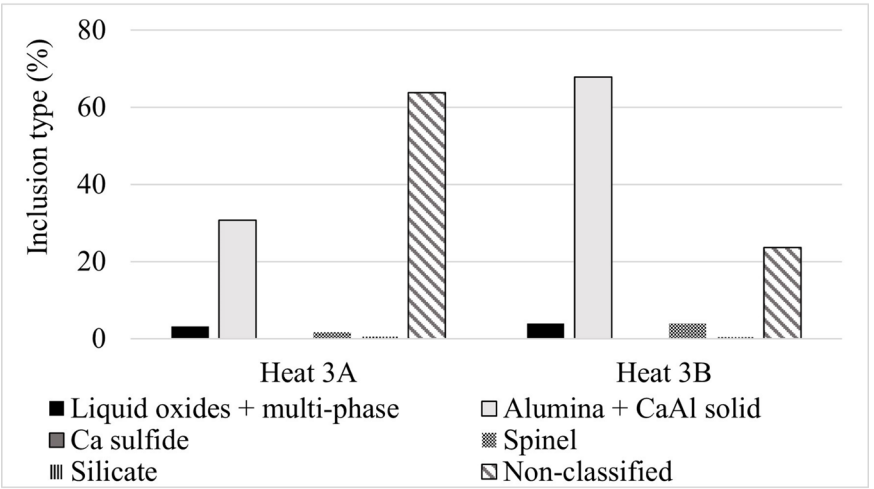

Figure 11. Distribution of inclusion types in tundish samples of heats 3A and 3B.

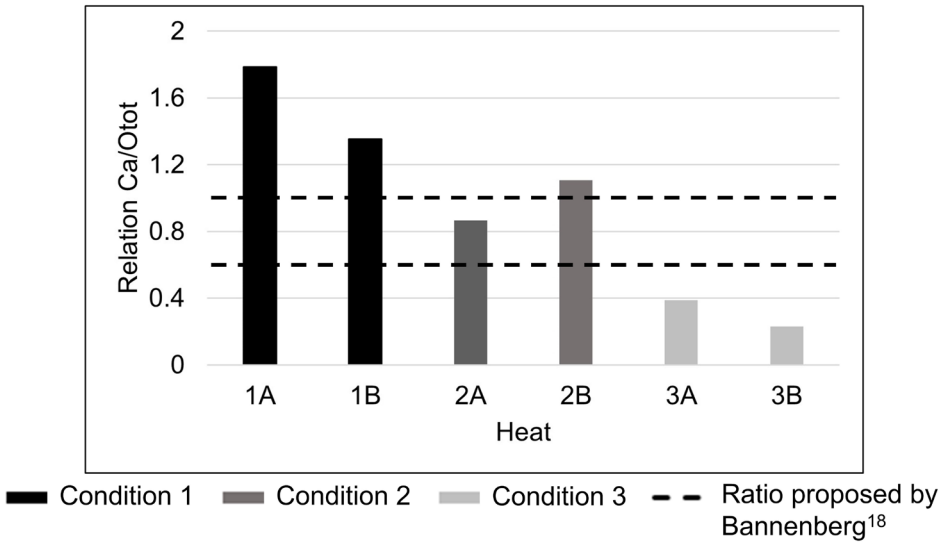

Figure 12. Ca/O_{total} in steel for tundish samples.

C3A or CaS. In both cases, nozzle clogging in continuous casting and quality loss[18,22] are to be expected with solid inclusions. CaS formation may be favored when sulfur levels are high in steel, which is not the case for the test heats. The maximum sulfur content found was 60 ppm, which suggests that CaS formation was mainly caused by excessive addition of calcium. The Ca/O_{total} ratio for this condition also indicates an excessive calcium addition. To achieve the optimum ratio proposed by Bannenberg[18], less calcium should be present.

The split addition condition showed the best results. Besides presenting lower inclusion density, it was the condition with the highest fraction of liquid and multi-phase inclusions in the tundish. There was no relevant CaS formation and the Ca/O_{total} meets the suggested range. Anticipating part of the calcium addition promoted a reduction in the final Ca content of the heats. This has the same practical effect as adding a smaller amount after RH, reaching the castability window. Another important fact is that the anticipation of Ca addition, as in conditions 2 and 3, implies a worsening of the alloy yield. Besides, the early addition may intensify the refractory wear in the vacuum chamber and RH snorkels, as reported by Poirier[23].

The injection condition only before the RH, although presenting an improvement in inclusion density compared to the standard injection condition (after RH), showed a majority of solid inclusions, rich in Al, and an insignificant number of liquid inclusions, which is unfavorable to the process.

All conditions showed a good correlation between computational thermodynamic calculations via Thermo-Calc + SLAG4 and the automated inclusion analysis results, which shows the importance of using the resource when the theme is inclusion modification through Ca addition.

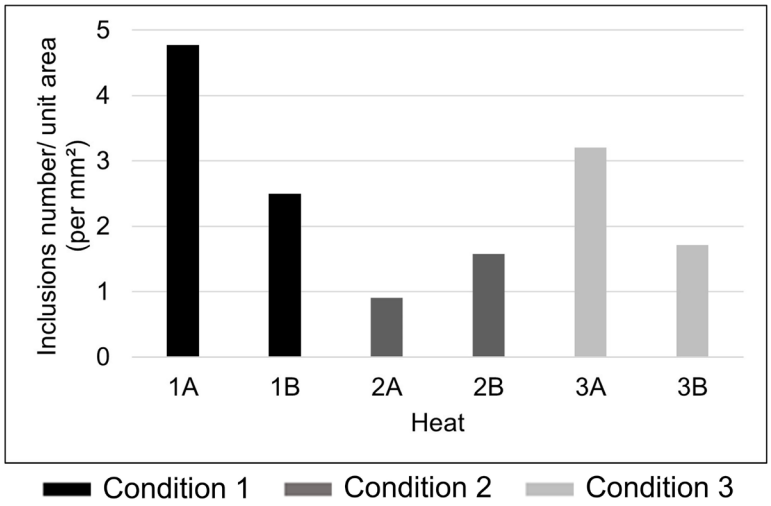

Figure 13. Inclusions density (inclusions number/mm^2) for tundish samples.

In all samples, non-classified inclusions represented a significant portion, indicating the need for refinement in the classification of these particles. One factor that may have contributed to the large amount of non-classified inclusions is the elevated Mn content, approximately 1.36 wt%, which probably led to the formation of MnS and (Ca,Mn)S inclusions. Our current classification methodology did not account for these types of particles. There is a need to incorporate more complex inclusion classification criteria in future studies. These criteria should account for associations of Mn and Ca sulfides linked to calcium aluminates, as reported by Choudhary and Ghosh[24]. Additionally, it is important to consider particles that are rich in microalloying elements such as titanium and niobium.

4. Conclusions

This study demonstrates that the timing of calcium addition during secondary refining significantly influences the efficiency of inclusion modification and, consequently, the cleanliness and castability of steel heavy plates.

Three alternative calcium addition timings were evaluated, namely: standard condition (all Ca after RH treatment), split condition (part of the Ca before and part after the RH treatment) and complete addition before the RH treatment.

The split condition proved to be the most effective in modifying inclusions, thus offering a promising approach for optimizing heavy plate steel production. The split addition of calcium resulted in a higher fraction of liquid and multi-phase inclusions and the lowest inclusion density, aligning closely with the calculated castability window. This condition minimized the formation of deleterious CaS inclusions and achieved a favorable Ca/O_{total} ratio.

In contrast, the standard addition condition led to excessive calcium levels, resulting in a higher prevalence of solid inclusions such as CaS and calcium aluminates, which are known to contribute to nozzle clogging during continuous casting.

The condition with calcium addition only before RH resulted in predominantly solid inclusions. The observed differences between conditions were closely related to how well each approach aligned with the castability window.

The correlation between computational thermodynamic simulations and the automated inclusion analysis underscores the reliability of using Thermo-Calc + SLAG4 as a predictive tool for inclusion behavior in steelmaking. These findings not only enhance the understanding of calcium treatment in steel production but also provide practical insights for optimizing calcium addition practices.

Although the split calcium addition was identified as the most effective condition for inclusion modification, future studies may benefit from exploring variations in the amount of calcium added, particularly reducing the calcium amount after the RH treatment. This adjustment could help prevent excessive calcium levels and minimize CaS formation. Furthermore, investigating early partial calcium additions may improve oxide inclusion modification, leading to more efficient inclusion removal and enhanced steel cleanliness. These approaches will be valuable for refining calcium addition strategies and optimizing heavy plate production.

5. Acknowledgments

The authors thank the teams from the Usiminas Research and Development Center and the Steelmaking Department for their support during this work and the support of the National Council for Scientific and Technological Development (CNPq).

6. References

1. Fan X, Zhang L, Ren Y, Yang W, Wu S. The effect of aluminum addition on the evolution of inclusions in an aluminum-killed calcium-treated steel. Metals (Basel). 2022;12(2):181-94. http://doi.org/10.3390/met12020181.
2. Ren Y, Wang W, Yang W, Zhang L. Modification of non-metallic inclusions in steel by calcium treatment: a review. ISIJ Int. 2023;63(12):1927-40. http://doi.org/10.2355/isijinternational.ISIJINT-2023-143.

3. Costa e Silva ALV. Non-metallic inclusions in steels – origin and control. J Mater Res Technol. 2018;7(3):283-99. http://doi.org/10.1016/j.jmrt.2018.04.003.
4. Pindar S, Pande MM. Formation mechanism, evolution and modification of nonmetallic inclusions in Alkilled, TiAlloyed Steel Melt: a review. Trans Indian Inst Met. 2023;76(10):2587-600. https://doi.org/10.1007/s12666-023-02947-9.
5. Basak S, Kumar Dhal R, Roy GG. Efficacy and recovery of calcium during CaSi cored wire injection in steel melts. Ironmak Steelmak. 2010;37(3):161-8. http://doi.org/10.1179/030192309X12506804200384.
6. Sanyal S, Panabaka M, Ghorui PK, Mishra D, Sambandam M. Experiences with calcium treatment of steel. In: 3rd International Conference on Science and Technology of Ironmaking and Steelmaking; 2017 Dec 11-13; Kanpur, India. Proceedings. India: Indian Institute of Technology Kanpur; 2017. p. 127-30.
7. Piva S, Assis AN, Pistorius PC, Kan M. Calciumtreated steel cleanliness prediction using highdimensional steelmaking process data. Integr Mater Manuf Innov. 2023;12(2):171-84. http://doi.org/10.1007/s40192-023-00300-y.
8. Holappa L, Hamalainem M, Liukkonen M, Lind M. Thermodynamic examination of inclusion modification and precipitation from calcium treatment to solidified steel. Ironmak Steelmak. 2003;30(2):111-5. http://doi.org/10.1179/030192303225001748.
9. Leão PBP, Klug JL, Carneiro CAR, Caldas H, Bielefeldt WV. Castability and inclusions in a low sulfur Ca-Treated peritectic steel for two deoxidation techniques. Steel Res Int. 2019;90(10):1-10. http://doi.org/10.1002/srin.201900151.
10. Turkdogan ET. Steel refining in the ladle. In: Turkdogan ET. Fundamentals of steelmaking. London: The Institute of Materials; 1996. p. 245-96.
11. Abraham S, Bodnar R, Raines J, Wang Y. Inclusion engineering and metallurgy of calcium treatment. J Iron Steel Res Int. 2018;25(2):133-45. http://doi.org/10.1007/s42243-018-0017-3.
12. Lu DZD. Kinetics, mechanisms and modelling of calcium treatment of steel [thesis]. Hamilton: McMaster University; 1992.
13. Soares FVD. Avaliação dos fatores que afetam a taxa de desnitrogenação no Desgaseificador a Vácuo RH para aços destinados a aplicação em Chapas Grossas [dissertation]. Belo Horizonte: Federal University of Minas Gerais; 2019.
14. Kaushik P, Lehmann J, Nadif M. State of the art in control of inclusions, their characterization, and future requirements. Metall Mater Trans, B, Process Metall Mater Proc Sci. 2012;43(4):710-25. http://doi.org/10.1007/s11663-012-9646-2.
15. Dogan N, Longbottom RJ, Reid MH, Chapman MW, Wilson P, Moore L, et al. Morphology and composition changes of spinel ($MgAl_2O_4$) inclusions in steel. Ironmak Steelmak. 2015;42(3):185-93. http://doi.org/10.1179/1743281214Y.0000000219.
16. Alves PC, Pereira JAM, Rocha VC, Bielefeldt WV, Vilela ACF. Avaliação da limpeza e reoxidação de um aço SAE 1055 modificado. In: 50th Steelmaking, Casting and Non-Ferrous Metallurgy Seminar. 2019 Oct 1-3; São Paulo, Brazil. Proceedings. São Paulo: ABM; 2019. p. 716-28. http://doi.org/10.5151/2594-5300-33780.
17. Bartosiaki BG, Pereira JAM, Bielefeldt WV, Vilela ACF. Assessment of inclusion analysis via manual and automated SEM and total oxygen content of steel. J Mater Res Technol. 2015;4(3):235-40. http://doi.org/10.1016/j.jmrt.2015.01.008.
18. Bannenberg N. Inclusion modification to prevent nozzle clogging. In: 78th Steelmaking Conference; 1995 Apr 2-5; Nashville, USA. Proceedings. Warrendale: Iron and Steel Society; 1995. p. 457-63.
19. Bai X, Sun Y, Chen R, Zhang Y, Cai Y. Formation and thermodynamics of CaS-bearing inclusions during Ca treatment in oil casting steels. Int J Miner Metall Mater. 2019;26(5):573-87. http://doi.org/10.1007/s12613-019-1766-0.
20. Wang L, Xi Z, Li C. Modification of type B inclusions by calcium treatment in high-carbon hard-wire steel. Metals (Basel). 2021;11(5):676-87. http://doi.org/10.3390/met11050676.
21. Lan F, Zhuang C, Li C, Yang G, Yao H. Effect of calcium treatment on inclusions in H08A welding rod steel. Metals (Basel). 2021;11(8):1227-39. http://doi.org/10.3390/met11081227.
22. Yang W, Zhang L, Ren Y, Chen W, Liu F. Formation and prevention of nozzle clogging during the continuous casting of steels: a review. ISIJ Int. 2024;64(1):1-20. http://doi.org/10.2355/isijinternational.ISIJINT-2023-376.
23. Poirier J. A review: influence of refractories on steel quality. Metall. Res. Technol. 2015;112(4):1-20. http://doi.org/10.1051/metal/2015028.
24. Choudhary SK, Ghosh A. Thermodynamic evaluation of formation of oxide–sulfide duplex inclusions in steel. ISIJ Int. 2008;48(11):1552-9. http://doi.org/10.2355/isijinternational.48.1552.